Research Article

Received: 30 July 2018 Revised: 25 September 2018 Accepted article published: 14 October 2018 Published online in Wiley Online Library: 20 November 2018

(wileyonlinelibrary.com) DOI 10.1002/jctb.5849

Ru-Sn-B/TiO_2 catalysts for methyl oleate selective hydrogenation. Influence of the preparation method and the chlorine content

María A Sánchez,[a] Vanina A Mazzieri,[a] Stéphane Pronier,[b] María A Vicerich,[a] Catherine Especel,[b] Florence Epron[b] and Carlos L Pieck[a*]

Abstract

BACKGROUND: Fatty alcohols are produced commercially by selective hydrogenation of fatty acid esters using copper-chromium catalysts. To reduce drastic reaction conditions, ruthenium-tin (Ru-Sn) catalysts reduced with sodium borohydride ($NaBH_4$) have been proposed. Chlorine (Cl) negatively affects the selectivity and activity of this catalytic system. To get further information on why Cl influences the selectivity negatively, this study investigated the influence of the preparation method on titania (TiO_2)-supported catalysts, which leads to catalysts with different Cl contents.

RESULTS: The activity and selectivity were greatly affected by the Cl content, which depends on the metal impregnation method (co-impregnation in excess of solution or co-impregnation by incipient wetness) and the support pre-calcination. Chlorine affects the Ru–Sn metal interaction, modifying the activity and selectivity. Catalysts with high Ru–Sn interaction are more selective to oleyl alcohol. Catalysts prepared by the co-impregnation method exhibit bigger particles than catalysts prepared by the incipient wetness method, with agglomerated Ru_3Sn_7 cubic phase of 50 nm surrounded by amorphous Ru-Sn.

CONCLUSION: High interaction between Ru and Sn is preferred because segregated Ru species are not selective for the formation of oleyl alcohol. The electronic state of Ru^0 is very important because small variations in the electron density lead to a decrease in the adsorption of hydrogen, or because Ru^0-H species do not have the adequate binding energy to produce the necessary 'hydride form'. The Ru electronic state is modified by the Cl that surrounds it, decreasing its ability to adsorb hydrogen.

Keywords: methyl oleate; selective hydrogenation; Ru-Sn-B/TiO_2 catalysts

INTRODUCTION

Fatty alcohols are important intermediates to produce surfactants, cosmetics and plasticizers.[1] In general, unsaturated fatty alcohols are more expensive than saturated alcohols because of the additional cost that the process requires to protect the unsaturated C=C double bond. In 1931, Adkins and Connor[2] discovered copper-chromium (Cu-Cr) catalytic systems for the hydrogenation of esters. Similar catalysts are still used for the hydrogenation of fatty acid esters but require high pressure of reaction (25–30 MPa). To reduce drastic reaction conditions, ruthenium-tin (Ru-Sn) catalysts reduced with sodium borohydride ($NaBH_4$) have been proposed.[3–7] In a previous work, we found that ruthenium-tin-boron/alumina (Ru-Sn-B/Al_2O_3) catalysts prepared by co-impregnation using the incipient wetness method had higher activity and selectivity than catalysts prepared by co-impregnation with excess solution.[8] Besides, catalysts prepared using $NaBH_4$ had high selectivity to oleyl alcohol, whereas Ru-Sn catalysts prepared without B were not selective for the formation of oleyl alcohol.[4] This behavior was attributed to different degrees of interaction between Ru and Sn.[4,9]

The support has a strong influence on the performances of the Ru-Sn catalysts used for selective hydrogenation of fatty acids or fatty esters to produce oleyl alcohol.[7,10,11] The support can strongly interact with the supported ruthenium oxide, affecting its reducibility, the size of the particles of Ru and the interaction between Ru and Sn.[11–13] In the case of a titania (TiO_2) support, the formation of a mixed oxide between Sn and TiO_2 was reported.[14,15] The catalytic properties of the support are also modified by chlorine (Cl) introduced by the metal precursors. In the case of the Ru-Sn/Al_2O_3 catalysts used for selective hydrogenation of fatty esters and fatty acids, it has been reported that the presence of Cl negatively affects the selectivity.[7,9,16] For other catalytic systems, the negative influence of Cl on the activity of Ru catalysts for carbon monoxide (CO) hydrogenation and CO and hydrogen (H_2) chemisorption was reported.[17,18] Also, the activity of Ru catalysts is significantly degraded by Cl in ammonia synthesis owing to its electron-withdrawing property.[19]

* Correspondence to: CL Pieck, INCAPE, Santa Fe, Argentina. E-mail: pieck@fiq.unl.edu.ar

a Instituto de Investigaciones en Catálisis y Petroquímica (INCAPE) (FIQ-UNL, CONICET), Santa Fe, Argentina

b Institut de Chimie des Milieux et des Matériaux de Poitiers (IC2MP), Université de Poitiers, UMR 7285 CNRS, Poitiers, France

In order to get further information on why Cl influences the selectivity negatively, we studied the effect of the preparation method on TiO_2-supported catalysts, which leads to catalysts with different Cl contents. Two preparation methods (co-impregnation with excess of impregnation solution and co-impregnation with the exact amount of impregnation solution, i.e. by incipient wetness) and two support pre-calcination temperatures (300 and 500 °C) were used.

EXPERIMENTAL

Catalyst preparation

Support preparation

TiO_2 was synthesized from $TiCl_4$ by the technique described previously.[20] One part was calcined at 300 °C and another part at 500 °C in a stream of dry air for 4 h to eliminate any contamination of organic compounds. The heating rate was 2 °C min^{-1}.

Preparation by co-impregnation method (CI) with excess solution

The catalyst was prepared according to the method described previously.[8] Metal precursors ($RuCl_3 \cdot xH_2O$ and $SnCl_2 \cdot 2H_2O$) as well as $NaBH_4$ were from Sigma Aldrich (St. Louis, USA) (>99% pure). Briefly, the support was impregnated with an aqueous solution containing the precursor salts of both metals (co-impregnation), adding an excess of solution. The solution was allowed to stand for 12 h, after which the samples were filtered and dried at 120 °C for 24 h in a stove. Then the metals were reduced with an aqueous solution of $NaBH_4$, filtered again, washed and dried at 120 °C for 4 h under nitrogen (N_2) blanketing. They were then reduced with H_2 at 300 °C for 2 h and cooled to room temperature in H_2. Finally, the system was flushed with N_2 and the catalyst was put in contact with air at room temperature.

Preparation by co-impregnation by incipient wetness method (IW)

The catalyst was prepared according to the method described previously.[11] Briefly, the support was wetted with exactly the pore volume of an aqueous solution of both metal precursor salts ($RuCl_3 \cdot 2H_2O$ and $SnCl_2 \cdot 2H_2O$) in the required amounts to achieve the desired metal content. Wetted samples were left to stand for 12 h, then reduced by the addition of aqueous $NaBH_4$, filtered, washed with water until neutrality and dried for 4 h at 120 °C under N_2 flow. Finally, the samples were reduced according to the same protocol as for CI catalyst.

The catalysts were called T °C-IW or T °C-CI, where T is the calcination temperature of the support (300 or 500 °C) and IW and CI are the methods of incorporation of metals (co-impregnation by incipient wetness or co-impregnation in excess solution respectively). The theoretical loadings of Ru and Sn were 1.5 and 3.0 wt% respectively using both preparation methods.

Characterization methods

Elemental analysis

The composition of the metal phase was determined by inductively coupled plasma optical emission spectroscopy (ICP-OES; Optima 2100 DV, Perkin Elmer) after digestion in an acid solution. The Cl content was determined spectrophotometrically by the mercury thiocyanate method using a Metrolab 1700 spectrophotometer.

Textural properties

The specific surface area (BET method), total pore volume and pore size distribution (BJH method) were determined by nitrogen adsorption. The catalyst samples were degassed at 200 °C for 2 h, then the nitrogen adsorption isotherm was determined at −196 °C with a Micromeritics ASAP 2020.

X-ray diffraction (XRD)

X-ray diffractograms were obtained with a Shimadzu XD-1 diffractometer (Cu Kα radiation filtered with Ni). The spectra were taken in the 2θ range between 20° and 70° at a sampling rate of 1.2° min^{-1}.

Temperature-programmed reduction (TPR)

The equipment (Ohkura TP 2002S) and conditions have been described elsewhere.[4] A known mass of catalyst was treated in air at 450 °C for 1 h, then cooled to room temperature under air flow. Then argon (Ar) was used for 15 min. Finally, a reducing mixture (5% H_2/Ar) was fed and the temperature was increased linearly from 25 to 700 °C at a rate of 10 °C min^{-1}.

Cyclohexane (CH) dehydrogenation

The reaction conditions and the method of analysis of the reaction products have been reported elsewhere.[4] In brief, the catalyst (50 mg) was charged and activated with H_2 (flow rate 36 mL min^{-1}) at 300 °C for 1 h before reaction. The reaction was carried out at 300 °C under atmospheric pressure and with a molar ratio H_2/CH = 30. Cyclohexane was provided by Sigma Aldrich (>99.9% pure).

X-ray photoelectron spectroscopy (XPS)

XPS measurements were carried out using a multi-technique system equipped with a dual Mg/Al X-ray source and a hemispherical PHOIBOS 150 analyzer (SPECS, Berlin, Germany) operating in fixed analyzer transmission (FAT) mode, following the technique described earlier.[4] The XPS analyses were performed on the solids after treatment with H_2/Ar at 300 °C. Calibration of the spectra was performed with the Ti $2p_{3/2}$ line (455 eV) from a TiO_2 support. Data treatment was performed with the Casa XPS program (Casa Software Ltd, Teignmouth, UK).[4]

Transmission electron microscopy (TEM)

The analyses were carried out with a Jeol JEM-2100 UHR microscope equipped with an Si(Li) detector for energy-dispersive X-ray (EDX) analysis and a Gatan Ultrascan 2k×2k camera. The samples were prepared in ethanol and placed in an ultrasonic bath without prior grinding. Fast Fourier transform (FFT) and electronic diffraction interpretations were performed using HighScore (XRD) software, the ICDD PDF-2 file for searching the sample phases, CaRIne Crystallography software to simulate the projection of diffraction patterns or FFTs, and IMAGE.J software to measure particle sizes for histograms. For each catalyst, approximately 500 metal particles were observed and the distribution of particle sizes was measured. The mean particle diameter (d_P) was calculated as

$$d_P = \sum n_i d_i^3 / \sum n_i d_i^2 \quad (1)$$

where n_i is the number of particles of diameter d_i.

Methyl oleate (9-octadecen-1-ol) hydrogenation

The experiments were carried out in a stainless steel autoclave reactor (280 cm^3 capacity). The reaction conditions (1 g of catalyst,

Table 1. Surface area, pore volume, pore size and average particle size determined for four studied catalysts

Physical property	300 °C-CI	500 °C-CI	300 °C-IW	500 °C-IW
Surface area (m^2 g^{-1})	93	38	103	48
Pore volume (cm^3 g^{-1})	0.21	0.22	0.25	0.25
Pore size (nm)	7.3	16.6	7.2	15.2
TiO_2 average particle size (nm)[a]	9	14	9	16

[a] Determined by XRD.

290 °C and 5 MPa) and the method for the analysis of the reaction products were reported previously.[21] In summary, reaction products were analyzed by gas chromatography (GC; Shimadzu GC-200) using a Zebron ZB-FFAP, Phenomenex, California, USA ZB-FFAP capillary column (length 30 m, inner diameter 0.25 mm) under the following conditions: injector temperature of 220 °C; column temperature of 200 °C for 1 min, 2 °C min^{-1} ramp up to 260 °C and then isothermal; detector (FID) temperature of 265 °C; N_2 carrier gas. Identification of reaction products was previously done by gas chromatography/mass spectrometry (GC/MS; Shimadzu QP-5000) using the same capillary column. Only oleyl alcohol, methyl stearate, stearyl alcohol and methyl oleate were detected as significant compounds in the reactor. The reagents (methyl oleate and *n*-dodecane) were provided by Sigma Aldrich (99% purity).

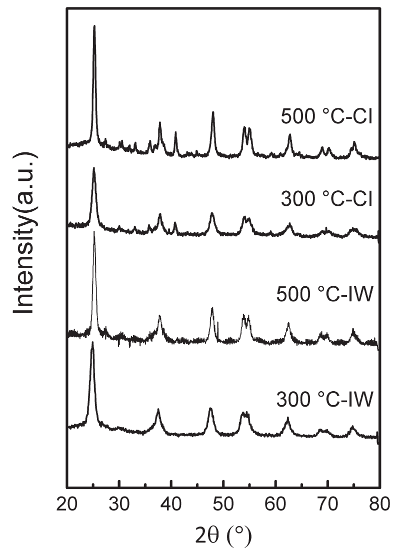

Figure 1. XRD patterns of catalysts prepared by IW and CI methods on TiO_2 support calcined at different temperatures.

Table 2. Ruthenium, Sn, B and Cl contents and cyclohexane conversion (CH) of TiO_2-supported catalysts prepared by different methods at different pre-calcination temperatures

Catalyst	Ru (wt%)	Sn (wt%)	B (wt%)	Cl (wt%)	CH (%)
300 °C-CI	1.29	2.86	0.32	0.42	6.8
500 °C-CI	1.27	2.76	0.20	0.35	3.0
300 °C-IW	1.28	2.97	0.31	0.32	6.1
500 °C-IW	1.26	2.92	0.18	0.29	2.7

RESULTS AND DISCUSSION

Table 1 shows the specific surface area, pore volume and pore size values of the studied catalysts. It is seen that the IW and CI catalysts for the supports calcined at 500 °C have pores almost twice the size of those calcined at 300 °C, while the surface area is strongly decreased (from 93 to 38 m^2 g^{-1} and from 103 to 48 m^2 g^{-1} for the CI and IW samples respectively). In order to determine whether the specific surface area modification is due to a change in the structure of the TiO_2 support, XRD analyses were performed on the catalysts. Rutile, anatase and brookite are the most common TiO_2 phases. Pure bulk anatase begins to transform irreversibly to rutile in air at about 600 °C; nevertheless, the transition temperatures vary between 400 and 1200 °C.[22] The wide XRD patterns (Fig. 1) of the samples display five TiO_2 diffraction lines centered at 25.3°, 37.8°, 48.0°, 54.9° and 62.8° corresponding to anatase crystal planes.[23] This means that the pre-calcination temperature or preparation method does not modify the support phase structure. However, the pre-calcination temperature of the support has an influence on the average particle size of TiO_2 anatase. As expected, the estimated average particle size of anatase determined by the Scherrer formula based on the diffraction peak at 25.3° is high on the support calcined at higher temperature, as can be seen in Table 1.

Table 2 displays the metal and Cl content and cyclohexane conversion values obtained for the four catalysts. For all catalysts, the Ru and Sn contents were slightly lower than the expected theoretical values of 1.5 and 3.0 wt% respectively. In addition, Table 2 shows that the catalyst prepared by a given method with the support calcined at 500 °C has a lower Cl content than the one prepared on the support calcined at 300 °C. This is because, during the calcination step, the support (TiO_2) gives off water, which entrains the residual Cl coming from the $TiCl_4$ precursor used for the preparation of the support. The higher the calcination temperature, the greater the water elimination and consequently the lower the amount of retained Cl. The IW method also produces catalysts with lower Cl contents, probably owing to the more efficient washing performed after the impregnation step of the metal precursors.

The TPR profiles of Ru and Sn monometallic catalysts supported on TiO_2 calcined at 500 °C were reported previously.[11] Boron was found to decrease the reduction temperature of Ru oxides from 128 to 110 °C, whereas the Sn oxides were reduced at a higher temperature, starting their reduction at 450 °C with a maximum around 600 °C. The shift in the Ru and Sn reduction temperature peaks shows that both metals were interacting with B. The electronegativity values of Ru, Sn and B are 2.20, 1.96 and 2.02 (Pauling) respectively. Therefore B is prone to give electrons to Ru and remove electrons from Sn. This could explain the different influence of B on the metal oxide reduction.

Figure 2 shows that for all bimetallic catalysts the maximum of the reduction peak of Ru oxides occurs at a higher temperature than for the Ru monometallic catalyst. This could be because the Sn is in strong interaction with the Ru, retarding the reduction. The Sn surface species would inhibit the contact of H with Ru atoms. In addition, when the support was calcined at 300 °C, a peak attributed to the reduction of segregated Sn species could

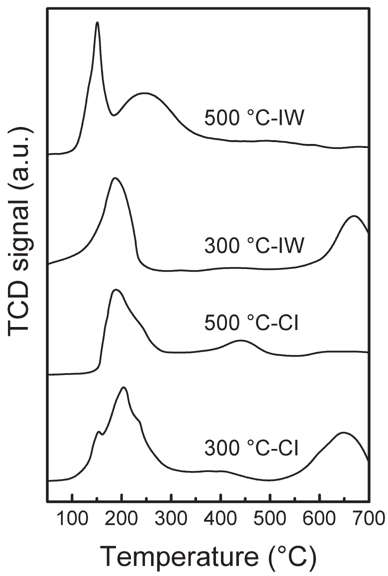

Figure 2. TPR profiles of catalysts prepared by IW and CI methods on TiO$_2$ support calcined at different temperatures.

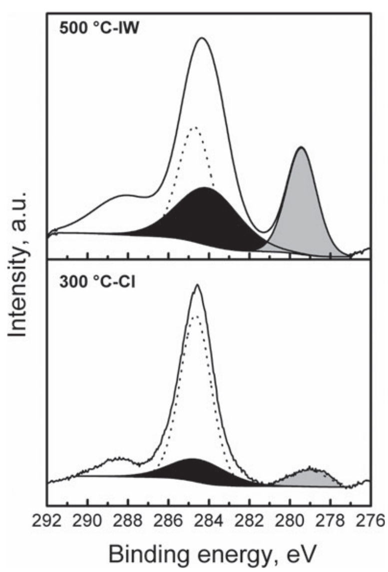

Figure 3. XPS spectra in Ru 3d region of 500 °C-IW and 300 °C-CI catalysts. Grey shaded peak, black shaded peak and dashed line correspond to Ru^0, Ru$^{\delta+}$ and C 1s respectively.

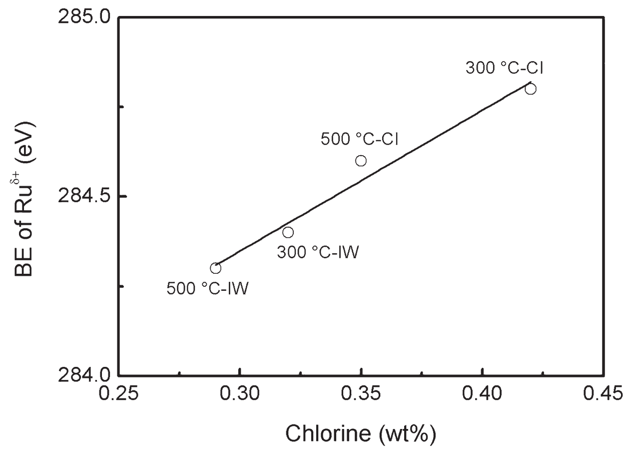

Figure 4. Binding energy of Ru$^{\delta+}$ species in Ru 3d$_{5/2}$ region as a function of chlorine content of catalysts.

Table 3. Surface atomic ratios of Ru and Sn species determined by XPS

Catalyst	Ru/Ti	Sn/Ti	Sn/Ru	Ru^0/(Ru$^{\delta+}$ + Ru^0)
300 °C-CI	0.053	0.364	6.87	0.33
500 °C-CI	0.031	0.279	9.00	0.55
300 °C-IW	0.068	0.474	6.97	0.48
500 °C-IW	0.062	0.305	4.92	0.79

be observed at a high temperature (>600 °C). When the support was calcined at 500 °C, Sn was reduced at a lower temperature (400 and 250 °C for the CI and IW catalysts respectively). This indicates that there are Sn oxide particles close to Ru whose reduction is catalyzed by Ru, especially for the IW sample. In conclusion, the TPR results show that for the support pre-calcined at 500 °C there are Ru, Sn and B species in strong interaction, the strongest Ru–Sn interaction being obtained in the IW catalyst. There are also more segregated Sn particles on the catalysts prepared with the support pre-calcined at 300 °C than on those prepared on the support pre-calcined at 500 °C.

Cyclohexane dehydrogenation is a useful reaction to measure the activity of the metallic function. Additional experiments with the monometallic Sn and Ru catalysts showed that only the monometallic Ru catalyst was active for cyclohexane dehydrogenation. On the one hand, it is widely known that the reaction is 'facile' (structure-insensitive) because it does not require a particular ensemble of neighboring metal atoms to form adsorbate bonds with the proper strength.[24,25] On the other hand, benzene is the only reaction product obtained in the reaction conditions used. Table 2 shows that the lower support pre-calcination temperature leads to catalysts with the highest values of cyclohexane conversion. In addition, by comparing catalysts with the same pre-calcination temperature, the IW ones lead to lower conversion values than the CI ones. Since Ru is active for the dehydrogenation of cyclohexane, while Sn is inactive, the lower activity of the IW catalysts could be due to a higher Ru–Sn interaction or simply because Ru accessibility is lower on the IW catalysts. Tin would decrease Ru activity because Sn deposited onto the Ru blocks the active sites (geometrical effect) or there are Sn atoms deposited near to Ru atoms which modify the electronic state of Ru, turning it less active (electronic effect). These results agree with the TPR profiles, since the support calcined at the lower temperature showed a higher amount of segregated Sn; consequently, the dehydrogenating activity of Ru was less affected by Sn. It is important to point out that there is no correlation between the Cl content of the catalysts and cyclohexane conversion, since the reaction is catalyzed by the metal function.

XPS analyses were performed to gain information about the electronic states of the surface Ru and Sn species. For the sake of simplicity, Fig. 3 only shows the XPS spectra of the bimetallic 500 °C-IW and 300 °C-CI catalysts, i.e. the best and worst catalysts in relation to the selectivity to oleyl alcohol. Figure 3 shows the 276–292 eV binding energy (BE) range where the peaks attributed to Ru are located. Since the C 1s peak at 284.6 eV of surface adventitious carbon overlaps with Ru 3d$_{3/2}$, the peak of Ru 3d$_{5/2}$ was employed

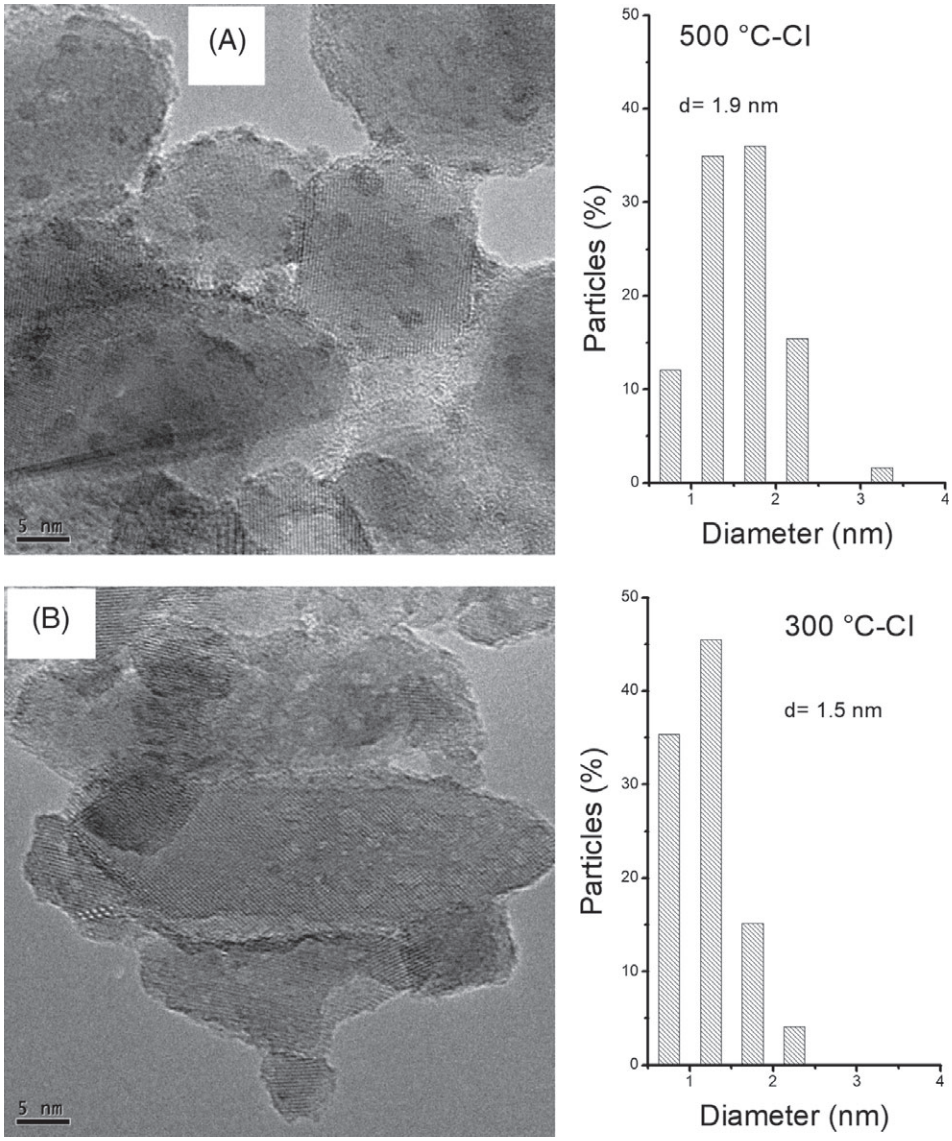

Figure 5. TEM images and particle size distributions of (A) 500 °C-Cl catalyst (630 particles analyzed) and (B) 300 °C-Cl catalyst (614 particles analyzed).

to determine the chemical state of Ru in all cases. To make the figure easier to analyze, only the Ru $3d_{5/2}$ peaks are shown. The XPS results show that Ru^0 metallic species are present in all catalysts, with BE values in the range between 279.2 and 280.1 eV, in accordance with the values for metallic Ru reported in the literature,[26–28] while the peak at 284.3–284.8 eV is attributed to Ru $3d_{5/2}$ oxidized species. The preparation method has an influence on the reduction of Ru because the $Ru^{\delta+}$ species of the catalysts prepared by the Cl method displayed BE values around 0.5 eV higher than those of the IW catalysts (Figs 3 and 4). These results are confirmed by a higher fraction of $Ru^0/(Ru^0 + Ru^{\delta+})$ for the IW catalysts as reported in Table 3. This phenomenon could be due to Cl deposited on the support because the increase in the BE of the $Ru^{\delta+}$ species correlates with the Cl content. Chlorine (electrophilic compound) would produce an increase in the BE of the $Ru^{\delta+}$ by inductive effect as seen in Fig. 4. The harmful effect of Cl on the reduction of Ru was also reported in the literature.[29–31] Mazzieri *et al.*[31] speculated that $Ru^{\delta+}$ species on these catalysts are associated with Cl species.

The low BE difference (<0.5 eV) between Sn^{2+} and Sn^{4+} species makes it almost impossible to distinguish them by XPS. A small peak in the range 484–485 eV and a greater peak at 486.1 eV were found for the Sn $3d_{5/2}$ band (results not shown). According to Rodina *et al.*,[32] the first peak can be attributed to Sn^0 and the second one to Sn^{n+} species. The $Sn^0/(Sn^0 + Sn^{n+})$ fraction is lower than 0.2 for all the catalysts. These results agree with those reported by other authors, since the complete reduction of Sn to the zero-valent state is very difficult to achieve.[33,34]

The Sn/Ti, Ru/Ti and Sn/Ru atomic ratios calculated from the elemental analysis are about 0.02, 0.01 and 1.92 respectively. The Sn/Ti and Ru/Ti surface atomic ratios obtained by XPS are displayed in Table 3. The catalysts prepared on the support calcined at 500 °C had lower Ru/Ti and Sn/Ti surface ratios than those prepared with the support calcined at 300 °C regardless of the preparation method used. Moreover, by comparing the catalysts prepared on the support calcined at the same temperature, the Cl catalysts had lower Ru/Ti and Sn/Ti surface atomic ratios than the IW ones. It is important to note that the Ru/Ti and Sn/Ti surface ratios are much higher than those expected from the bulk analysis, in agreement

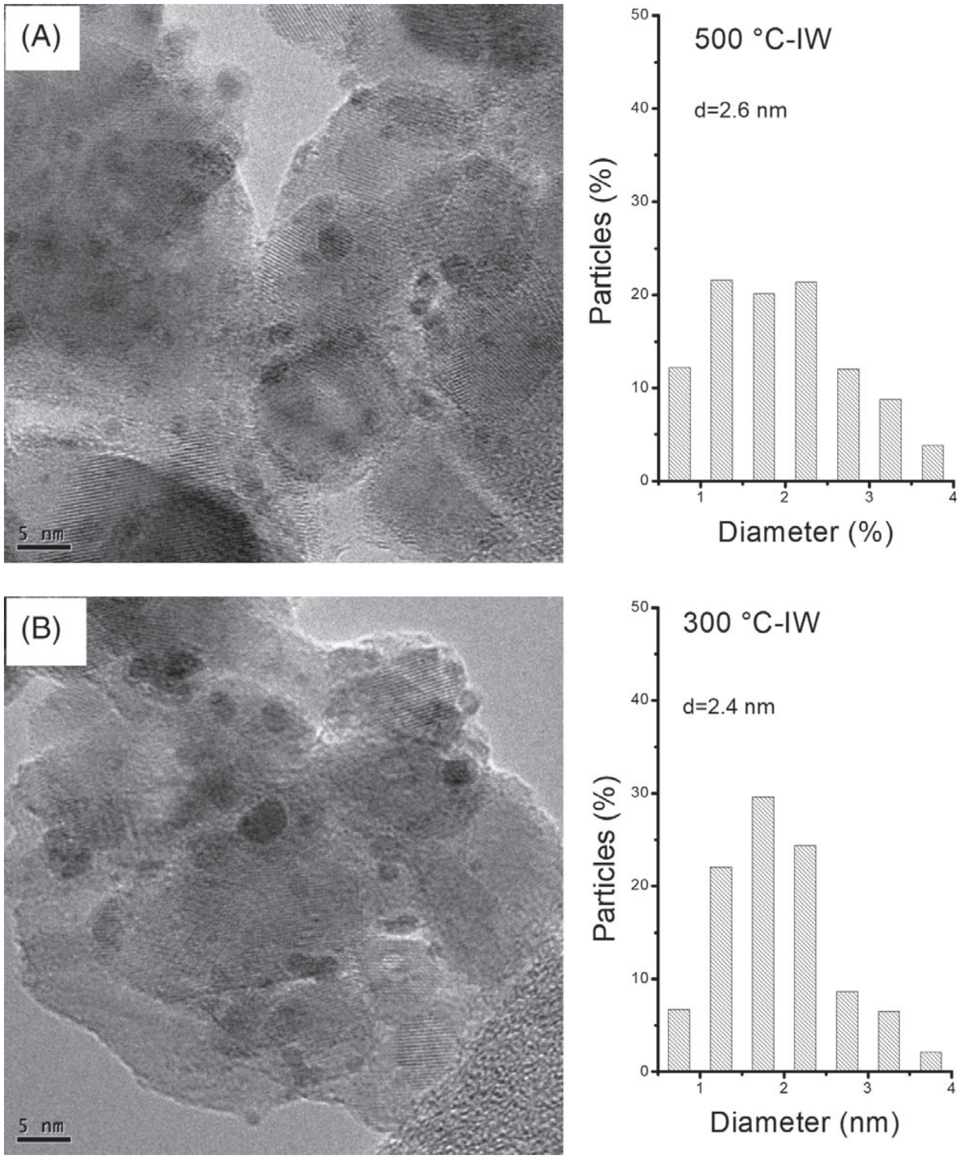

Figure 6. TEM images and particle size distributions of (A) 500 °C-IW catalyst (491 particles analyzed) and (B) 300 °C-IW catalyst (476 particles analyzed).

with the results reported by Gu *et al.*[35] and Elmasides *et al.*[36] For a 2% Ru/TiO_2 catalyst after reduction at 550 °C, Elmasides *et al.*[36] reported that the surface was dramatically enriched in Ru, with a Ru/Ti surface ratio > 1. Similar results were found for Ru-Sn/Al_2O_3 catalysts, since Rodina *et al.*[32] reported that the Sn/Al and Ru/Al surface ratios were ten and four times bigger than the bulk atomic ratios respectively. The Sn/Ru surface ratio was also higher than the bulk ratio.

XPS data (not shown) indicated a decrease in the amount of chlorinated species at higher calcination temperature in accordance with the values reported in Table 1.

An exhaustive analysis of the samples by TEM and EDX was performed. On the 500 °C-CI catalyst, crystallized Ru-Sn phase agglomerates of 50 nm were observed. The EDX analyses showed a very homogeneous ratio of Sn/Ru = 7/3. The images in FFT and High-angle annular dark-field (HAADF) imaging confirmed the presence of a Ru_3Sn_7 phase of cubic structure. Also, small particles (Sn and Ru phase) and characteristic Sn oxide particles with their 'great distance' (d_{hk1} = 0.3359 nm for plane (110) of tetragonal SnO_2) were observed. There are areas consisting essentially of SnO_2.

On the 300 °C-CI catalyst, Ru-Sn phase agglomerates, corresponding to Ru_3Sn_7, of about 50 nm but less well crystallized and more numerous than on the 500 °C-CI catalyst were found. Also, EDX analyses, FFT images as well as HAADF imaging confirmed the presence of Ru_3Sn_7 phase of cubic structure. There were also very small particles dispersed on TiO_2 for which the diffraction was very difficult to obtain and whose EDX detection was low with a Sn/Ru ratio of about 4/1. Some particles of Sn oxide were also detected. Complementary large analysis on dispersed particles showed that Sn/Ru ratios were between 90/10 and 80/20, therefore with higher Sn contents than on the 500 °C-CI catalyst.

In the case of the 500 °C-IW catalyst, very small agglomerates of $RuSn_2$ phase with particles size of 5 nm were observed. This phase can only be observed in electronic diffraction since it seems to be covered by an amorphous phase containing Ru and Sn. There were also dispersed particles on the support with sizes between 4 and 5 nm (atomic Sn/Ru ratio between 10/90 and 20/80) and between 2 and 3 nm (with metallic contents very variable, Sn/Ru atomic ratio between 70/30 and 20/80). The electron diffractions demonstrated that the observed phases are tetragonal $RuSn_2$ and Ru_3Sn_7.

TEM and EDX analysis of the 300 °C-IW catalyst showed agglomerated particles of about 30 nm of Ru-Sn phase less crystallized than on the 300 °C-CI catalyst. These particles have a Sn/Ru atomic ratio between 3/7 and 1/1. It is also possible to observe small particles of about 1–4 nm gathering hexagonal or cubic Ru, tetragonal SnO_2 or cubic Ru_3Sn_7 phases. It is important to point out that the 'wide analyses' showed that the Sn/Ru ratios are 30/70 or 80/20. Therefore the bimetallic particles are very heterogeneous. Also, particles dispersed on TiO_2 with atomic Sn/Ru ratio of about 5/95 were found by EDX analyses.

It should be noted that in all the catalysts there was a difference between the Sn/Ru ratios determined by the crystallographic structures and the EDX analyses. This could be explained by the fact that the particles are crystallized but they undoubtedly contain an amorphous surrounded Ru-Sn metal phase. The 'wide analysis' by EDX of the surface shows that the Sn/Ru atomic ratio on the IW catalysts is lower than on the CI catalysts.

Figures 5 and 6 show typical TEM images and metal size distributions corresponding to CI and IW catalysts respectively. It is important to point out that the big agglomerates of about 30–50 nm were not considered for calculating the metal size distribution, which probably leads to an underestimation of the mean metallic particle size, especially on CI catalysts.

Figure 7 shows the methyl oleate conversion as a function of the reaction time. All the catalysts showed a similar initial activity. Differences in catalytic activity started to be marked at about 60 min. Catalysts with high cyclohexane dehydrogenation activity also had high hydrogenation activity to convert methyl oleate (Table 2 and Fig. 7), except for the 500 °C-IW catalyst, which presents the lowest cyclohexane conversion but the highest methyl oleate one at the end of the reaction. This might indicate that both reactions take place on different active sites. Cyclohexane dehydrogenation occurs on surface Ru, while Sn is inactive and even negatively affects the Ru activity by an electronic or geometric effect. The geometric effect involves the blocking of active Ru ensembles by the added modifier atoms. The electronic effect corresponds to the modification of the Ru electronic density due to an interaction with Sn neighboring atoms. Such electronic modification would in turn change the adsorption energy of the chemical species participating in the catalytic reaction. It has been proved that both effects are important.[37,38] Moreover, the hydrogenation of methyl oleate is catalyzed by Ru and Sn in strong interaction.[4,6,28,39–41] More recently, Rodina *et al.*[32] proposed that crystalline Ru_xSn_y structures with variable composition were the active component of the selective hydrogenation catalyst. The high activity was attributed to Ru^0 sites interacting with Sn^{2+} or Sn^{4+} Lewis acid sites.[6] It is also possible that the lower Cl content of the 500 °C-IW catalyst favors the conversion of methyl oleate because Cl decreases the Ru–Sn interaction.[7,9]

Figure 8 shows conversion values at the end of the reaction as a function of the Sn/Ru atomic ratio obtained by XPS. As the Sn/Ru ratio increases, the catalyst appears to be less active. At high Sn/Ru ratios, Sn could encapsulate Ru and thereby block its catalytic activity. Figure 9 shows values of selectivity to oleyl alcohol (desired product) as a function of reaction time. As expected, selectivity goes through a maximum as a function of the reaction time since oleyl alcohol is an intermediate reaction product, being transformed to stearyl alcohol at higher reaction times. Sn/Ru

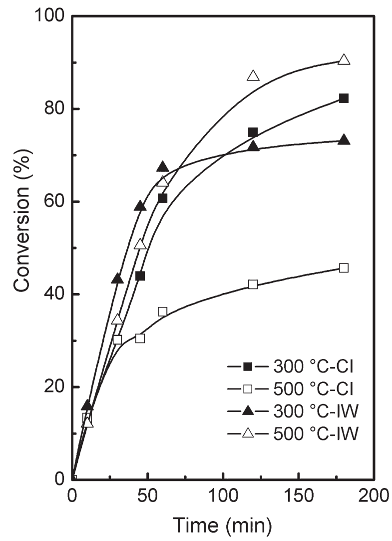

Figure 7. Conversion of methyl oleate as a function of reaction time obtained with four studied catalysts.

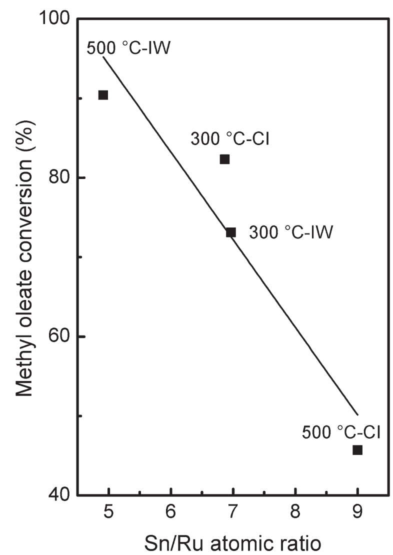

Figure 8. Conversion of methyl oleate at 180 min reaction time as a function of Sn/Ru atomic ratio obtained by XPS.

atomic ratios equal to 2 or 4 have been reported as the optimal values favoring the formation of the unsaturated alcohol.[3,7,28,41] The values reported in Table 3 show that the prepared catalysts have a Sn/Ru surface ratio much higher than the optimum. By EDX analysis, it was found that only the catalyst 500 °C-IW, the most selective to oleyl alcohol, displays the $RuSn_2$ tetragonal phase.

In addition, catalysts prepared with the support previously calcined at 500 °C are seen to be more selective to the desired product (oleyl alcohol) than those prepared with the support calcined at 300 °C regardless of the preparation method. As previously reported, good selectivity to oleyl alcohol is achieved when there is a strong Ru–Sn interaction. TPR and cyclohexane dehydrogenation have shown that a previous calcination of the support at 500 °C leads to a strong Ru–Sn interaction, probably due to the elimination of Cl. Echeverri *et al.*[9] have reported that Cl prevents a strong interaction between Ru and Sn species, thus leading to catalysts with low selectivity to oleyl alcohol.

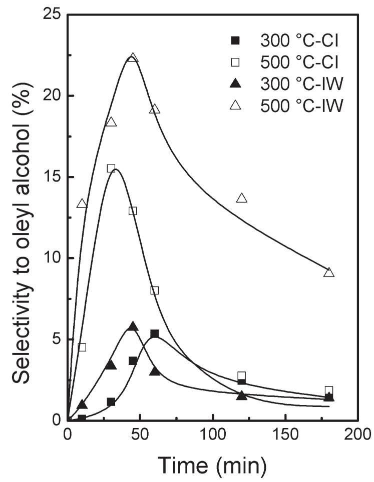

Figure 9. Selectivity to oleyl alcohol as a function of reaction time obtained with four studied catalysts.

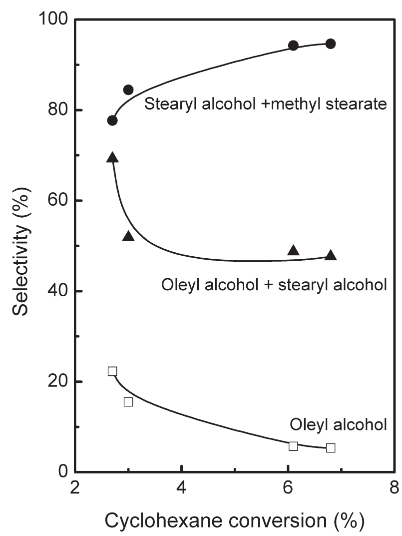

Figure 10. Selectivity to oleyl alcohol, sum of selectivities to stearyl alcohol and methyl stearate and sum of selectivities to oleyl alcohol and stearyl alcohol as a function of conversion of cyclohexane (values taken at maximum selectivity to oleyl alcohol).

Figure 10 shows the selectivity to oleyl alcohol, the sum of the selectivities to stearyl alcohol and methyl stearate and the sum of the selectivities to oleyl alcohol and stearyl alcohol as a function of the activity for dehydrogenation cyclohexane. With the increase in the cyclohexane dehydrogenation activity, the selectivity to oleyl alcohol decreases as well as the selectivity to oleyl alcohol + stearyl alcohol. This can be explained by considering that cyclohexane dehydrogenation is catalyzed by Ru, while the selective hydrogenation of methyl oleate to oleyl alcohol occurs on Ru species in strong interaction with Sn. Besides, the sum of the selectivities to stearyl alcohol and methyl stearate, i.e. the selectivity for hydrogenation of the C=C double bond, increases with the cyclohexane dehydrogenation activity. This indicates that isolated Ru preferably hydrogenates the C=C double bond.

Figure 11 shows the maximum selectivity to oleyl alcohol obtained in each catalyst as a function of the Cl content. The higher selectivity to oleyl alcohol is obtained on the catalyst of lower Cl content. However, this correlation is not linear and after

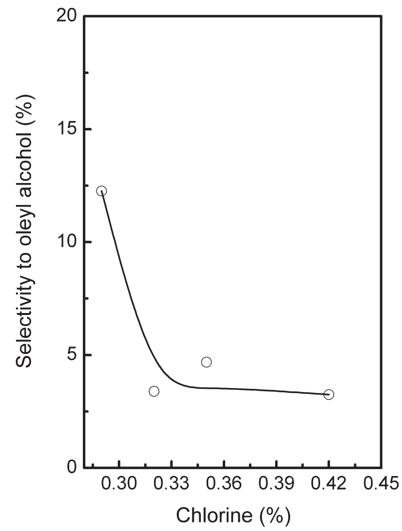

Figure 11. Maximum selectivity to oleyl alcohol obtained in each catalyst as a function of chlorine content.

a certain threshold value the ability to produce oleyl alcohol remains constant.

To explain the results, it is necessary to analyze the reaction mechanism and the active sites involved in the reaction. The reaction mechanism proposed for the selective hydrogenation of methyl oleate to oleyl alcohol is direct hydrogenation or stepwise hydrogenation via the formation of an aldehyde intermediate.[6,28] In both mechanisms, the oxygen of the C=O group is bonded to Sn oxide species which must be in strong interaction with Ru.[3,6,7,28] A similar model was proposed for the Ru-Sn-B/TiO_2 catalyst where the Sn oxide species are replaced by Ti^{3+} species.[12] Basically, the direct hydrogenation mechanism proposes that electron-rich Ru^0 activates the H_2 into a 'hydride form'. Sn^{2+} or Sn^{4+} Lewis acid sites, which are in interaction with Ru, polarize the carbonyl of the ester, facilitating the hydrogen transfer from an adjacent Ru-H site. The hydrogen activated on Ru attacks the carbon atom of the carbonyl groups and an acetal of Sn is formed.

The Cl present in the support would modify the electronic state of Ru, mainly of the Ru oxidized species (changing the BE; see Fig. 4). By inductive effect, the electronic state of the Ru^0 is also changed. Moreover, Cl inhibits the reduction of Ru to the metallic state (Table 3). Therefore the adsorption of hydrogen on Ru^0 is disturbed. This alters the attack by the hydrogen of the carbon atom of the carbonyl group, thus leading to a lower selectivity to alcohol. The active sites for the reaction proposed by several researchers are formed by Sn and Ru in strong interaction with Sn/Ru atomic ratio of 2.[3,7,41] The TEM and EDX results showed that the 500 °C-IW catalyst, the most selective to oleyl alcohol, possesses the highest amount of $RuSn_2$ tetragonal phase, and big agglomerates of Ru_3Sn_7 phase were not observed.

The main advantage of the Ru-Sn-B/TiO_2 catalyst in comparison with the commercial copper chromite catalyst is the drastic reduction of the working pressure to 3–5 MPa, while the reaction temperature is similar. The commercial processes also have a higher yield to stearyl alcohol.[21] However, a higher yield to fatty alcohol could be obtained in our case by optimizing the reaction conditions, especially the residence time, because stearyl alcohol is the final reaction product. In this sense, high selectivity to stearyl alcohol could be obtained at high values of residence time in a continuous reactor. Long residence times would be obtained at high values of the catalyst mass to feed flowrate ratio.

CONCLUSIONS

It was found that the activity and selectivity were greatly affected by the Cl content, which depends on the metal impregnation method (co-impregnation by incipient wetness or in excess solvent) and the support pre-calcination treatment. It has been proved that it is better to pre-treat the support at high temperature (500 °C) to remove more Cl to obtain more selective catalysts.

The electronic state of Ru^0 is very important because small variations in the electron density lead to a decrease in the adsorption of the hydrogen. This electronic state is modified by the Cl surrounding the Ru atoms.

Catalysts prepared by the CI method exhibit bigger agglomerated Ru_3Sn_7 cubic phase of 50 nm surrounded by amorphous Ru-Sn than those prepared by the IW method. However, big agglomerates are also found on the 300 °C-IW catalyst but they are smaller (30 nm). The 500 °C-IW catalyst does not present big agglomerates. CI catalysts present a bimodal particle size distribution, with small particles lower than 2.5 nm and agglomerates of 50 nm. The wide analysis by EDX of the surface shows that the Sn/Ru atomic ratio determined on the IW catalysts is lower than on the CI catalysts.

The experimental results clearly show that sites involved in the hydrogenation of methyl oleate and in the dehydrogenation of cyclohexane are different.

ACKNOWLEDGEMENTS

This work had the financial support of Consejo Nacional de Investigaciones Científicas y Técnicas and Universidad Nacional del Litoral (Project CAI+D), Argentina.

REFERENCES

1 Knaut J and Richtler HJ, Trends in industrial uses of palm and lauric oils. *J Am Oil Chem Soc* **62**:317–327 (1985).
2 Adkins H and Connor R, The catalytic hydrogenation of organic compounds over copper chromite. *J Am Chem Soc* **53**:1091–1095 (1931).
3 Narasimhan CS, Deshpande VM and Ramnarayan K, Selective hydrogenation of methyl oleate to oleyl alcohol on mixed ruthenium–tin boride catalysts. *Appl Catal* **48**:L1–L6 (1989).
4 Sánchez MA, Mazzieri VA, Sad MR, Grau R and Pieck CL, Influence of preparation method and boron addition on the metal function properties of Ru–Sn catalysts for selective carbonyl hydrogenation. *J Chem Technol Biotechnol* **86**:447–453 (2011).
5 Piccirilli A, Pouilloux Y, Pronier S and Barrault J, Selective hydrogenation of methyl oleate into oleyl alcohol in the presence of ruthenium-tin-supported catalysts. *Bull Soc Chim Fr* **132**:1109–1117 (1995).
6 Deshpande VM, Ramnarayan K and Narasimhan CS, Studies on ruthenium-tin boride catalysts II. Hydrogenation of fatty acid esters to fatty alcohols. *J Catal* **121**:174–182 (1990).
7 Cheah KY, Tang TS, Mizukami F, Niwa S, Toba M and Choo YM, Selective hydrogenation of oleic acid to 9-octadecen-1-ol: catalyst preparation and optimum reaction conditions. *J Am Oil Chem Soc* **69**:410–416 (1992).
8 Sánchez MA, Mazzieri VA, Sad MR and Pieck CL, Influence of the operating conditions and kinetic analysis of the selective hydrogenation of methyl oleate on Ru–Sn–B/Al_2O_3 catalysts. *React Kinet Mech Catal* **107**:127–139 (2012).
9 Echeverri DA, Marín JM, Restrepo GM and Rios LA, Characterization and carbonylic hydrogenation of methyl oleate over Ru-Sn/Al_2O_3: effects of metal precursor and chlorine removal. *Appl Catal Gen* **366**:342–347 (2009).
10 Mendes MJ, Santos OAA, Jordão E and Silva AM, Hydrogenation of oleic acid over ruthenium catalysts. *Appl Catal Gen* **217**:253–262 (2001).
11 Sánchez MA, Mazzieri VA, Vicerich MA, Vera CR and Pieck CL, Influence of the support material on the activity and selectivity of Ru–Sn–B catalysts for the selective hydrogenation of methyl oleate. *Ind Eng Chem Res* **54**:6845–6854 (2015).
12 Corradini SAdS, Lenzi GG, Lenzi MK, Soares CMF and Santos OAA, Characterization and hydrogenation of methyl oleate over Ru/TiO_2, Ru–Sn/TiO_2 catalysts. *J Non Cryst Solids* **354**:4865–4870 (2008).
13 Bond GC, Preparation and properties of vanadia/titania monolayer catalysts. *Appl Catal Gen* **157**:91–103 (1997).
14 Oliveira MM, Schnitzler DC and Zarbin AJG, (Ti,Sn)O_2 mixed oxides nanoparticles obtained by the sol–gel route. *Chem Mater* **15**:1903–1909 (2003).
15 Lin J, Yu JC, Lo D and Lam SK, Photocatalytic activity of rutile $Ti_{1-x}Sn_xO_2$ solid solutions. *J Catal* **183**:368–372 (1999).
16 Ishii K, Mizukami F, Niwa S, Toba M, Ushijima H and Sato T, Effects of raw materials and preparation methods of catalysts on the selective hydrogenation of ethyl phenylacetate. *J Am Oil Chem Soc* **73**:465–469 (1996).
17 Ragaini V, Carli R, Bianchi CL, Lorenzetti D and Vergani G, Fischer–Tropsch synthesis on alumina-supported ruthenium catalysts I. Influence of K and Cl modifiers. *Appl Catal Gen* **139**:17–29 (1996).
18 Narita T, Miura H, Ohira M, Hondou H, Sugiyama K, Matsuda T *et al.*, The effect of reduction temperature on the chemisorptive properties of Ru/Al_2O_3: effect of chlorine. *Appl Catal* **32**:185–190 (1987).
19 Li J, Kitano M, Ye T-N, Sasase M, Yokoyama T and Hosono H, Chlorine-tolerant ruthenium catalyst derived using the unique anion-exchange properties of 12 CaO·7 Al_2O_3 for ammonia synthesis. *ChemCatChem* **9**:3078–3083 (2017).
20 Benítez VM, Yori JC, Vera CR, Pieck CL, Grau JM and Parera JM, Characterization of transition-metal oxides promoted with oxoanions by means of test reactions. *Ind Eng Chem Res* **44**:1716–1721 (2005).
21 Sánchez MA, Mazzieri VA, Oportus M, Reyes P and Pieck CL, Influence of Ge content on the activity of Ru–Ge-B/Al_2O_3 catalysts for selective hydrogenation of methyl oleate to oleyl alcohol. *Catal Today* **213**:81–86 (2013).
22 Hanaor DAH and Sorrell CC, Review of the anatase to rutile phase transformation. *J Mater Sci* **46**:855–874 (2011).
23 Wu L, Yu JC, Wang X, Zhang L and Yu J, Characterization of mesoporous nanocrystalline TiO_2 photocatalysts synthesized via a sol-solvothermal process at a low temperature. *J Solid State Chem* **178**:321–328 (2005).
24 Gault FG, Mechanisms of skeletal isomerization of hydrocarbons on metals. *Adv Catal* **30**:1–95 (1981).
25 Boudart M, Aldag A, Benson JE, Dougharty VA and Harkings CG, On the specific activity of platinum catalysts. *J Catal* **6**:92–99 (1966).
26 Xie S, Qiao M, Li H, Wang W and Deng J-F, A novel Ru–B/SiO_2 amorphous catalyst used in benzene-selective hydrogenation. *Appl Catal Gen* **176**:129–134 (1999).
27 Moulder JF, Stickle WF, Sobol PE and Bomben KD, *Handbook of X-ray Photoelectron Spectroscopy*, ed. by Chastain J. Perkin-Elmer Corporation, Minnesota, USA (1992).
28 Pouilloux Y, Autin F, Guimon C and Barrault J, Hydrogenation of fatty esters over ruthenium–tin catalysts; characterization and identification of active centers. *J Catal* **176**:215–224 (1998).
29 Van Der Steen PJ and Scholten JJF, Selectivity to cyclohexene in the gas phase hydrogenation of benzene over ruthenium, as influenced by reaction modifiers: II. Catalytic hydrogenation of benzene to cyclohexene and cyclohexane. *Appl Catal* **58**:291–304 (1990).
30 Milone C, Neri G, Donato A, Musolino MG and Mercadante L, Selective hydrogenation of benzene to cyclohexene on Ru/γ-Al_2O_3. *J Catal* **159**:253–258 (1996).
31 Mazzieri VA, Coloma-Pascual F, Arcoya A, L'Argentière PC and Fígoli NS, XPS, FTIR and TPR characterization of Ru/Al_2O_3 catalysts. *Appl Surf Sci* **210**:222–230 (2003).
32 Rodina VO, Ermakov DY, Saraev AA, Reshetnikov SI and Yakovlev VA, Influence of reaction conditions and kinetic analysis of the selective hydrogenation of oleic acid toward fatty alcohols on Ru-Sn-B/Al_2O_3 in the flow reactor. *Appl Catal Environ* **209**:611–620 (2017).
33 Adkins SR and Davis BH, The chemical state of tin in platinum-tin-alumina catalysts. *J Catal* **89**:371–379 (1984).
34 Sexton BA, Hughes AE and Foger K, An X-ray photoelectron spectroscopy and reaction study of Pt-Sn catalysts. *J Catal* **88**:466–477 (1984).

35 Gu Q, Long J, Fan L, Chen L, Zhao L, Lin H *et al.*, Single-site Sn-grafted Ru/TiO_2 photocatalysts for biomass reforming: synergistic effect of dual co-catalysts and molecular mechanism. *J Catal* **303**:141–155 (2013).
36 Elmasides C, Kondarides DI, Grünert W and Verykios XE, *XPS and FTIR study of Ru/Al_2O_3 and Ru/TiO_2 catalysts: reduction characteristics and interaction with a methane–oxygen mixture. J Phys Chem B* **103**: 5227–5239 (1999).
37 Parera JM and Fígoli NS, Reactions in the commercial reformer, in *Catalytic Naphtha Reforming: Science and Technology*, ed. by Antos GJ, Aitani AM and Parera JM. Marcel Dekker, New York, NY, pp. 45–78 (1995).
38 Edgar MD, Catalytic reforming of naphtha in petroleum refineries, in *Applied Industrial Catalysis*, ed. by Leach BE. Academic Press, New York, NY, pp. 123–148 (1983).
39 Luo G, Yan S, Qiao M, Zhuang J and Fan K, Effect of tin on Ru-B/γ-Al_2O_3 catalyst for the hydrogenation of ethyl lactate to 1,2-propanediol. *Appl Catal Gen* **275**:95–102 (2004).
40 Pouilloux Y, Piccirilli A and Barrault J, Selective hydrogenation into oleyl alcohol of methyl oleate in the presence of Ru-SnAl_2O_3 catalysts. *J Mol Catal Chem* **108**:161–166 (1996).
41 Sánchez MA, Mazzieri VA, Vicerich MA, Vera CR and Pieck CL, Ru-Sn-B/Al_2O_3 catalysts for selective hydrogenation of methyl oleate: influence of the Ru/Sn ratio. *J Chem* **2015**:561350 (2015).

